

## Rheological and flow characteristics of nanofluids: Influence of electroviscous effects and particle agglomeration

K. B. Anoop, S. Kabelac, T. Sundararajan, and Sarit K. Das

Citation: *Journal of Applied Physics* **106**, 034909 (2009); doi: 10.1063/1.3182807

View online: <http://dx.doi.org/10.1063/1.3182807>

View Table of Contents: <http://scitation.aip.org/content/aip/journal/jap/106/3?ver=pdfcov>

Published by the [AIP Publishing](#)

---

### Articles you may be interested in

[Giant electrorheological effect in Fe<sub>2</sub>O<sub>3</sub> nanofluids under low dc electric fields](#)

*J. Appl. Phys.* **108**, 034306 (2010); 10.1063/1.3462445

[Effects of shear rate and temperature on viscosity of alumina polyalphaolefins nanofluids](#)

*J. Appl. Phys.* **107**, 054317 (2010); 10.1063/1.3309478

[Particle shape effects on thermophysical properties of alumina nanofluids](#)

*J. Appl. Phys.* **106**, 014304 (2009); 10.1063/1.3155999

[Response to "Comment on 'Particle concentration and tube size dependence of viscosities of Al<sub>2</sub>O<sub>3</sub>-water nanofluids flowing through micro- and minitubes'" \[Appl. Phys. Lett.94, 066101 \(2009\)\]](#)

*Appl. Phys. Lett.* **94**, 066102 (2009); 10.1063/1.3078394

[Comment on "Particle concentration and tube size dependence of viscosities of Al<sub>2</sub>O<sub>3</sub>—water nanofluids flowing through micro- and minitubes" \[Appl. Phys. Lett.91, 243112 \(2007\)\]](#)

*Appl. Phys. Lett.* **94**, 066101 (2009); 10.1063/1.3078393

---



## Re-register for Table of Content Alerts

Create a profile.



Sign up today!



# Rheological and flow characteristics of nanofluids: Influence of electroviscous effects and particle agglomeration

K. B. Anoop,<sup>1</sup> S. Kabelac,<sup>2</sup> T. Sundararajan,<sup>1</sup> and Sarit K. Das<sup>1,a)</sup>

<sup>1</sup>*Department of Mechanical Engineering, Indian Institute of Technology Madras, Chennai 600036, India*

<sup>2</sup>*Institute for Thermodynamics, Helmut Schmidt University (University of the Federal Armed Forces Hamburg), Holstenhofweg 85, Hamburg 22043, Germany*

(Received 30 April 2009; accepted 20 June 2009; published online 10 August 2009)

Nanofluids have shown remarkable attraction in heat transfer community due to its reported enhanced thermal properties. One factor which can restrict nanofluids in heat transfer application is the increased viscosity value (compared to classical predictions). Particle aggregation occurring was the major reason for this observation. Even though majority of the aqueous nanofluids prepared in literature were stabilized electrostatically by adjusting the *pH*, studies on the effect of the electrical double layer thus created and its influence on viscosity increase has not been investigated for these nanofluids so far. Thus, in the present paper, rheological properties of alumina-water nanofluids, which are electrostatically stabilized, are measured and the increase in suspension viscosity due to presence of this electrical double layer causing additional electroviscous effects is brought out. Based on dynamic light scattering studies, particle agglomeration and its subsequent effect in increasing the viscosity of alumina-ethylene glycol nanofluid, where electroviscous effects are absent, are also considered. It is noted that the understanding of electroviscous effect is equally important as understanding the particle agglomeration effect and understanding both the effects is central to revealing the physics of nanofluid rheology. Further, hydrodynamic experiments are made, which show that nanofluids behaves almost like a homogeneous fluids under flow conditions, and by knowing their properties, such as viscosity and density, pressure drop can be predicted.

© 2009 American Institute of Physics. [DOI: [10.1063/1.3182807](https://doi.org/10.1063/1.3182807)]

## I. INTRODUCTION

Nanofluids, which are dilute colloidal dispersions of nanosized particles in a fluid, have exhibited some advantageous features such as improved heat transfer, longer shelf life, and control of suspension stability. However, accommodation of these advantages into practical applications, such as engine cooling, electronic chip cooling, heat exchangers, and laser assisted drug delivery, requires a collective analysis of both heat transfer as well as flow properties. Effective viscosity of nanofluid is one among the dominant property as it governs the ease of flow, pressure drop, and the consequent pumping power involved during flow applications. Recently, many researchers<sup>1–10</sup> investigated the rheological behaviors of nanofluids. Many observations showed Newtonian behavior under low particle loading<sup>1–5</sup> nanofluids, while a shear thinning nature was shown for nanofluids with higher particle loading [above 10 vol % (Ref. 6)] as well as for oil-based nanofluids.<sup>7</sup> It was also reported that the viscosity values were significantly higher than the classical prediction theories for dilute suspensions. Aggregations of particles were primarily the reason for the above observation. Even though majority of the aqueous nanofluids prepared<sup>4,5,9,10</sup> were stabilized electrostatically by adjusting the *pH*, discussion on the effect of the electrical double layer thus created and its influence on viscosity increase have not been investigated for nanofluids so far. Thus in the present work, an effort to understand the influence of additional electroviscous

effects due to presence of an electrical double layer caused by electrostatic stabilization process in increasing the suspension viscosity is made theoretically. Three types of nanofluids, viz., alumina-water, alumina-ethylene glycol, and copper oxide-ethylene glycol are considered for the investigation. Alumina-water nanofluids are stabilized by adjusting the *pH* value far away from isoelectric point (IEP) and no stabilizers added to any of the nanofluids as it may induce undesired effects in viscosity values.

## II. EXPERIMENTAL

### A. Preparation of nanofluids

Nanofluids used in the present study were prepared by a top-down approach. By this two categories of nanofluids were produced. Category 1 corresponds to nanofluids prepared by dispersing nanopowder bought from different powder manufactures in a base fluid and category 2 belongs to nanofluids procured as such in dispersion either in concentrated form or at a fixed low concentration. The concentrated nanofluids were diluted with the base fluid when necessary. Alumina-water and CuO-ethylene glycol nanofluid formulated by diluting concentrated nanofluid (40 wt %) procured from Nanophase, Inc., are denoted by Al<sub>2</sub>O<sub>3</sub>-water\_NP and CuO-EG\_NP, whereas alumina-water and alumina-ethylene glycol nanofluid prepared by dispersing nanopowder procured from Sigma Aldrich are denoted by Al<sub>2</sub>O<sub>3</sub>-water\_SA and Al<sub>2</sub>O<sub>3</sub>-EG\_SA, respectively, in the present communication. Four basic steps were involved in the preparation of the above nanofluids. (a) After mixing nanopowder in a base

<sup>a)</sup>Electronic mail: skdas@iitm.ac.in.

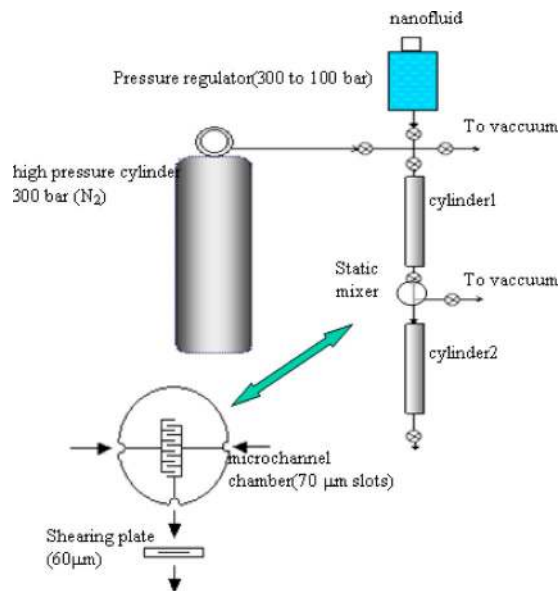


FIG. 1. (Color online) Schematic of high pressure shearing setup.

fluid (or diluting the concentrated nanofluid with base fluid), the suspension was homogenized using a high performance disperser/stirrer (T25 digital ULTRA-TURRAX) for around 30 min, whereby the nanofluid was thoroughly mixed in a turbulent motion through a rotor and stator structure. (b) The above solution was further kept in an Ultrasonic bath (35 kHz) for about 2 h. Here microturbulences caused by fluctuation of pressure and cavitations imparted energy for deagglomeration of particles to its basic sizes. (c) Following this, a high power ultrasonication using an Ultrasonic disruptor (KLN Sys 587), which was inserted into the nanofluid solution, was carried out for about 1 h. The disruptor consisted of a probe attached to a sonotrode, vibrating at 20 kHz and 50  $\mu\text{m}$  amplitude. The temperature of the nanofluid during the process of sonication was maintained at 22  $^{\circ}\text{C}$  by external cooling. (d) Further deagglomeration was carried out by passing the suspension through a high pressure shearing process, whose significance in nanofluid production was previously noted by some researchers.<sup>11,12</sup> For this purpose, a high pressure static mixer [Combi-mixer (101-10001-F) Ehrfeld Mikrotechnik BTS GmbH] which was basically consist of a chamber made of microchannels (with gap of 70  $\mu\text{m}$  each) through which the fluid passes and the final shearing occurring through a shearing plate of 60  $\mu\text{m}$  width has been used. Deagglomeration happens mainly due to high shear forces as well as due to strong impact occurring in the microchannel chamber. The working pressure of about 100 bars, provided by a high pressure nitrogen cylinder, maintains the high pressure shearing flow. A schematic of the above setup is shown in Fig. 1.

Five different volume fractions of 0.5, 1, 2, 4, and 6 vol % are considered for the analysis. Particle size distribution by percentage intensity, as well as number measured using a Malvern Zetasizer Nano-ZS90 for alumina-water nanofluid ( $\text{Al}_2\text{O}_3$ -water\_SA) prepared by the above dispersion procedure [Sigma Aldrich powder (No. 544833) with size of  $<50$  nm and surface area of 35–43  $\text{m}^2/\text{g}$ ], is shown in Fig. 2. Transmission electron microscopy (TEM) of the

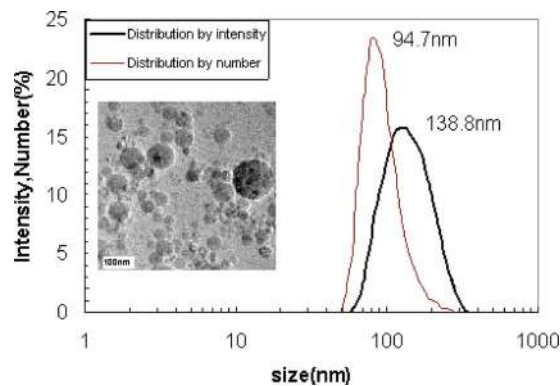


FIG. 2. (Color online) Particle size distribution for alumina-water nanofluid (alumina-water\_SA).

particles (obtained from a JEM 3010) is given in the inset which shows the primary spherical morphology and sizes of particles. As seen, the average particle diameter obtained is around 100 nm, which is larger than the primary particle size as claimed by the powder suppliers (50 nm), indicating that some agglomeration also occurs while suspending particles in base fluid. During experimentation, the  $\text{pH}$  value of the above alumina-water nanofluid is maintained at around 4.5 (the IEP  $\text{pH}$  value for alumina-water nanofluid<sup>13</sup> is around 8.9) which gives a zeta-potential value of 54 mV, assuring good electrostatic stability. The particle size distribution got by dynamic light scattering (DLS) method for diluted alumina-water nanofluid (named as  $\text{Al}_2\text{O}_3$ -water\_NP) from Nanophase (Nanotek A1112W, particle size of  $\sim 50$  nm) also showed similar behavior as that of  $\text{Al}_2\text{O}_3$ -water\_SA nanofluid obtained by dispersing Sigma Aldrich alumina powder in water. The concentrated nanofluid purchased was diluted using de-ionized water and the average particle size and zeta-potential obtained were 95 nm and 58 mV (at  $\text{pH}=4.3$ ), respectively. Copper oxide nanofluid in ethylene glycol (diluted from 40 wt % dispersion, Nanophase, named as  $\text{CuO}$ -EG\_NP) showed an average size of 152 nm.

## B. Viscosity measurements

Viscosities of nanofluid samples prepared by the procedure described above are measured using a Physica UDS 200 rheometer having a cone and plate geometry (cone diameter of 75 mm and a cone angle of  $1^{\circ}$ ). All experiments are conducted at a constant gap of 0.05 mm and an initial stabilization period of 2 min is given for achieving constant temperature, after which a variable shear rate ranging from 10/s to 1000/s is applied. As the torque applied during the experiment is in the range of 1–150  $\mu\text{N m}$ , the percentage error in viscosity measurement as specified for the equipment is limited to 2%. Water and ethylene glycol, the base fluids used, show a Newtonian behavior with viscosity values of approximately 1 and 21 mPa s, respectively, in the shear rate range of 10–1000  $\text{s}^{-1}$  at 20  $^{\circ}\text{C}$ , which practically matches with their theoretical values. The viscosity ratio (the ratio of the viscosity of nanofluid to that of base fluid) versus shear rate for the nanofluids presently studied is plotted, as shown in Fig. 3. It is seen that with an increase in the particle concentration, the viscosity ratio increases and this increase seems

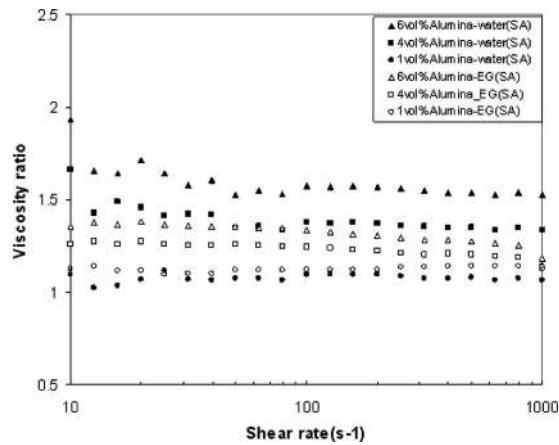


FIG. 3. Viscosity ratio variation with shear rate for alumina-water and alumina-ethylene glycol nanofluids.

to be more predominant for water-based nanofluids than for ethylene glycol-based ones. Newtonian behavior is also exhibited for both water-based as well as ethylene glycol-based nanofluids in the above shear rate regime. Figures 4(a) and 4(b) show the variation in nanofluid viscosities with temperature at a constant shear rate of  $200 \text{ s}^{-1}$ . It may be seen here that the viscosities of the base fluid as well as that of nanofluids decrease with an increase in temperature. Interestingly, it may be noticed that at  $50 \text{ }^\circ\text{C}$ , the viscosity of 6 vol % alumina nanofluid becomes almost equal to the viscosity of water at  $20 \text{ }^\circ\text{C}$ . The above observation reveals the fact that an inappropriate use of viscosity value may give rise to misleading results in pumping power and heat transfer char-

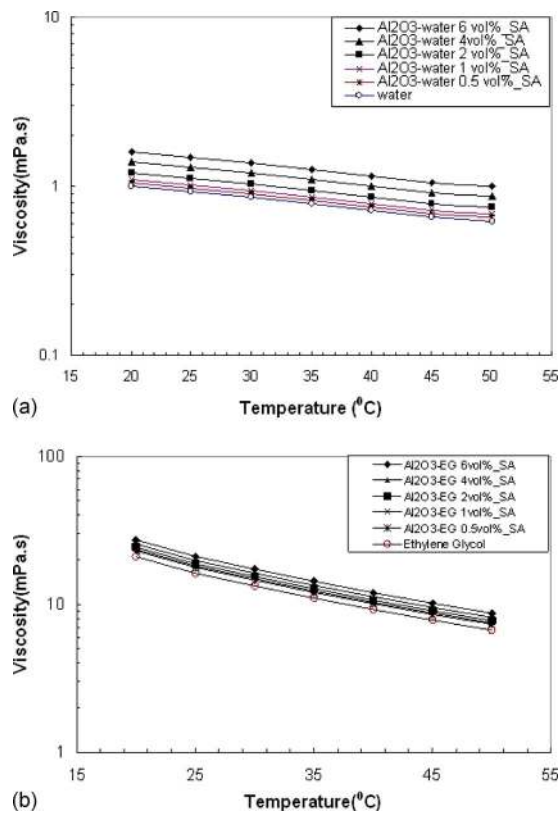


FIG. 4. (Color online) Viscosity variation with temperature for alumina-water and alumina-ethylene glycol nanofluids.

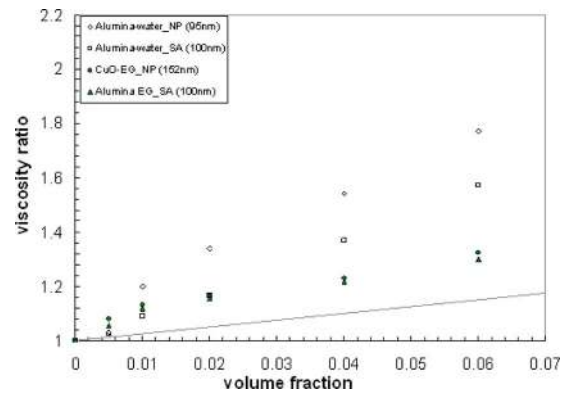


FIG. 5. (Color online) Viscosity ratio variation with particle concentration for nanofluids.

acteristics as they are highly dependent on fluid properties. Comparing Figs. 4(a) and 4(b), it may be also noticed that the effect of temperature in the reduction in viscosity is more severe for ethylene glycol-based nanofluids than for water-based ones. During experimentation, it was observed that CuO-ethylene glycol nanofluid exhibited more agglomeration than alumina-ethylene glycol nanofluids which necessitated frequent ultrasonication to maintain a uniform dispersion. However, the trends in rheological behaviors (viscosity variation with shear rate and temperature) for other nanofluids, namely,  $\text{Al}_2\text{O}_3$ -water\_NP and CuO-EG\_NP are observed to be similar as that explained above and a detailed description is not presented here. So as to compare the viscosity enhancement observed, an increment in viscosity for all nanofluids studied compared to their base fluids is depicted in Fig. 5. Here the relative viscosity values are plotted against volume fraction at a given temperature of  $20 \text{ }^\circ\text{C}$  and shear rate of  $200 \text{ s}^{-1}$ . A comparison with the theoretical prediction by Einstein's equation [Eq. (2), given later] is also plotted in the figure.

Theoretically, viscosity ratios of colloidal suspensions or nanofluids are generally written in a power series form<sup>14</sup> with volume fraction  $\phi$  as

$$\frac{\eta_{\text{nf}}}{\eta_{\text{bf}}} = 1 + [\eta]\phi + K[\eta]^2\phi^2 + O(\phi)^3 + \dots \quad (1)$$

Here  $\eta_{\text{nf}}$  and  $\eta_{\text{bf}}$  indicate the viscosity of the nanofluid and the base fluid, respectively, the term  $[\eta]$  is generally referred to as the intrinsic viscosity and  $K$  is Huggins' coefficient. It is seen that the presence of solid particles in a fluid always introduces additional disturbances in flow, distorting the flow field, and giving rise to an increase in the dissipation of energy. The  $\phi$  term in the above equation takes care of such disturbances,<sup>15</sup> whereas the  $\phi^2$  term accounts for the effect of pair interactions between suspended particles.<sup>14</sup> Since particle concentration below 10 vol % is considered in the present study, the effect of  $\phi^2$  term and hence Huggins coefficient may not be of much significance as particle-particle interactions primarily occurs at higher particle concentrations. For a suspension of uncharged particles, intrinsic viscosity value is determined by the geometry of the suspended particles (e.g., the value of  $[\eta]$  for spherical particles is 2.5). Thus neglecting higher order terms, Eq. (1) reduces to

$$\frac{\eta_{nf}}{\eta_{bf}} = 1 + 2.5\phi, \quad (2)$$

which is popularly known as Einstein's equation for dilute suspensions. As seen from Fig. 5, the experimental viscosity values of nanofluids are found to be much more than that of the base fluid as well as that of theoretical predictions. It is also observed that the increment in viscosity ratio is not so linear at lower concentrations but becomes linear toward higher concentrations. Many researchers attributed particle agglomeration as the cause for the observed increment in viscosity above the conventional theoretical predictions. It is seen that at a fixed particle concentration, alumina-water nanofluids exhibit higher viscosity ratios than alumina-ethylene glycol nanofluids. Assuming similar trends in particle agglomeration for both water-based and ethylene glycol-based nanofluids, one aspect that differentiates the two nanofluids is the fact that the former is stabilized electrostatically by adjusting the  $pH$ , while the latter is not. Hence, the influence of electrostatic stabilization procedure on the viscosity of nanofluids needs to be investigated and a theoretical reasoning needs to be proposed.

### C. Theoretical explanation

It is to be noted that the intrinsic viscosity value of 2.5 in Einstein's equation holds good only when the particles are uncharged. Since in the present case nanofluids are electrostatically stabilized, the presence of an electrical double layer introduces additional increase in viscosity brought about by electroviscous forces, in contrast to the case when particles do not have surface charges. These additional effects on  $[\eta]$  and  $K$  are known as the primary and the secondary electroviscous effects, respectively. Thus, the intrinsic viscosity value for suspensions may be now modified and written as<sup>16</sup>

$$[\eta]_{EV} = [\eta](1 + p). \quad (3)$$

Here  $[\eta]_{EV}$  denotes the intrinsic viscosity value when electroviscous forces are present,  $[\eta]$  is the intrinsic viscosity value with uncharged particles, and  $p$  is the primary viscous coefficient. It may be noted that this coefficient basically gives the percentage increment in intrinsic viscosity. Rigorous mathematical formulations were done in the past to evaluate  $p$ , starting with Smoluchowski,<sup>17</sup> followed by many researchers.<sup>18–20</sup> Adachi *et al.*<sup>16</sup> in their studies with dilute suspensions of sodium montmorillonite showed that the value of  $p$  would be proportional to  $\kappa^{-1}$ , which is the double layer thickness, also known as Debye length. In their model it is proposed that the increment in viscosity is due to the effective excluded volume due to electrical double layer. The schematic of an additional volume arising due to the presence of an ionic cloud, as described above, is shown in Fig. 6(a). Considering spherical particles with radius  $r$  surrounded by an ionic layer of thickness  $\kappa^{-1}$ , the increment in viscosity due to the excluded volume of the ionic cloud, which can be correlated with the primary viscous coefficient,  $p$  is expressed as<sup>16</sup>

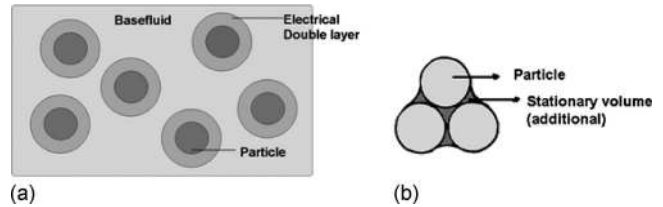


FIG. 6. (a) Schematic depicting increase in effective volume when an electrical double layer is present over the particle surface. (b) Schematic showing the presence of immobile additional liquid volume when particle aggregation occurs.

$$p = \frac{(r + \kappa^{-1})^3 - r^3}{r^3}. \quad (4)$$

For evaluating  $p$ , the double layer thickness has to be evaluated. The Debye length for an electrolytic solution is given by

$$\kappa^{-1} = \sqrt{\frac{\epsilon_0 \epsilon_r k_B T}{2N_A e^2 I}}, \quad (5)$$

where  $\epsilon_0$  is the permittivity of free space ( $8.854 \times 10^{-12} \text{ C}^2 \text{ N}^{-1} \text{ m}^{-2}$ ),  $\epsilon_r$  is the dielectric constant (for water, 78.4),  $k_B$  is Boltzmann's constant,  $T$  is the absolute temperature (300 K),  $N_A$  is Avogadro's number,  $e$  is the elementary charge ( $1.602 \times 10^{-19}$ ), and  $I$  is the ionic strength (moles/ $\text{m}^3$ ). When monovalent ions are present in the solution as in present case (with HCl acid only added to control the  $pH$ ), the above equation reduces to<sup>21</sup>

$$\kappa^{-1} = (32.87 \times 10^8 \sqrt{I})^{-1}. \quad (6)$$

The evaluation of ionic strength in a colloidal suspension is not straightforward, and an estimation following the hypothesis laid down by Rubio-Hernández *et al.*<sup>22</sup> is adopted in the present analysis. Rubio-Hernández *et al.*<sup>22</sup> proposed that the surface charge on a particle is entirely screened or neutralized at the IEP and there is no electrical double layer that surrounds the particles at this  $pH$  value. Thus the difference in  $pH$  value of the suspension from the isoelectric  $pH$  value (i.e.,  $\Delta pH = pH - pH_{IEP}$ ) may be used for evaluation of ionic strength. This indirectly suggests that the ionic cloud around the particle will be more prominent as the suspension  $pH$  is away from the isoelectric  $pH$  value. Converting this  $\Delta pH$  into ionic strength or moles/l (for, e.g., when  $\Delta pH = 3$ ,  $I = 10^{-\Delta pH}$  moles/l =  $1000 \times 10^{-3}$  moles/ $\text{m}^3$ ) and substituting it in Eq. (6), an approximate estimate of double layer thickness can be made. Figure 7 shows the variation in the double layer thickness with respect to the  $pH$  of a suspension, assuming the IEP is 8.7. In the present study, the  $pH$  of alumina-water nanofluid was maintained approximately at around 4.5, and so the value of  $\kappa^{-1}$  will be around 40 nm. This distance determines the distance at which the particles feel each others presence and may be noted to be depending only on the properties of the suspending medium. Now plotting the  $p$  values (primary viscous coefficient) for different particle sizes as a function of  $pH$ , it may be noted that this electroviscous coefficient will be lying between 2 and 4 (Fig. 8). Assuming an average value of 3 for  $p$ , the intrinsic vis-

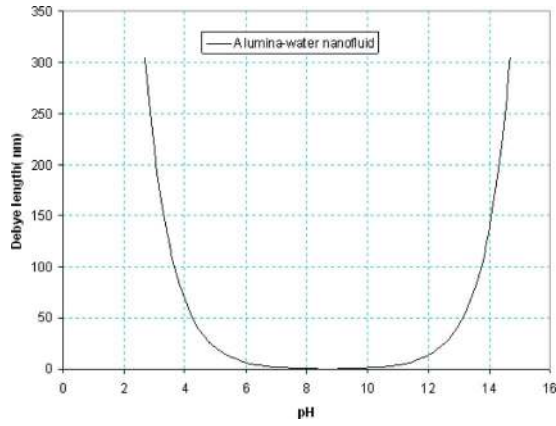


FIG. 7. (Color online) Electrical double layer thickness as a function of pH.

cosity with primary viscous effects may be evaluated from Eq. (3) as

$$[\eta]_{EV} = [\eta](1 + p) = 2.5(1 + 3) = 10. \tag{7}$$

It may be also noted from Fig. 8 that the value of  $p$  and hence the viscosity may be higher for suspensions containing smaller particles than for suspensions with larger particle sizes. Including the primary viscous forces, the relative viscosity for alumina-water-based nanofluids will take the form

$$\frac{\eta_{nf}}{\eta_{bf}} = 1 + 10\phi. \tag{8}$$

As mentioned earlier, another important factor that can increase the viscosity of nanofluids is the aggregation of particles in the suspension. It may be noted that when particle aggregates are formed, they also include some stationary volume of the fluid [Fig. 6(b)], which, in fact, increases the effective volume. The aggregation factor is also evident from the DLS studies (Fig. 2) which show the average particle sizes for alumina nanopowders to be around 100 nm even though the basic particle sizes were less than 50 nm (as seen from TEM). Thus, assuming a maximum increase in the volume fraction by a factor of 2 (which is the ratio of the aggregated particle size to the basic particle size), the relative viscosity may be written as

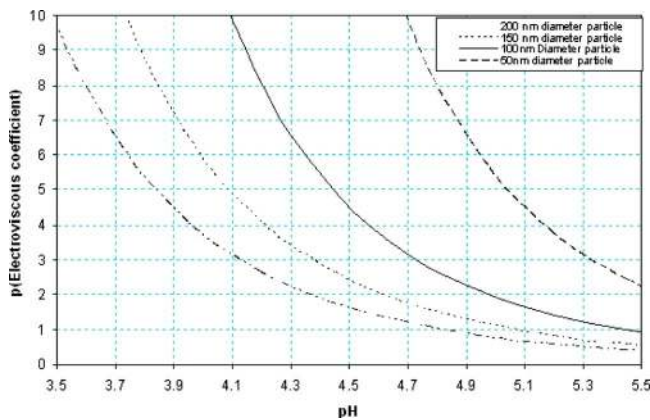


FIG. 8. (Color online) Primary electroviscous coefficient  $p$  as a function of pH.

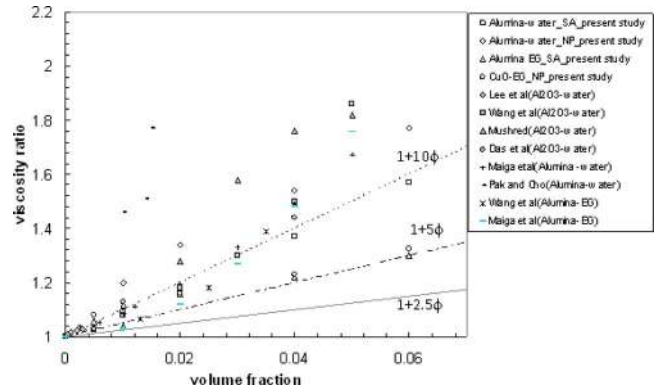


FIG. 9. (Color online) Viscosity ratio variation with particle concentration for nanofluids studied as well as data from literature for alumina based nanofluids.

$$\frac{\eta_{nf}}{\eta_{bf}} = 1 + 2.5\phi \times 2 = 1 + 5\phi. \tag{9}$$

The above explanation can answer the increase in viscosity values for ethylene glycol-based nanofluids where no electrical double layers are formed as pH was not controlled to maintain stability.

Now the experimental data from the present study, along with results from literatures,<sup>1,4,5,8–10</sup> are plotted in Fig. 9. It is seen that the theoretical predictions considering electroviscous effects [Eq. (8)] are able to predict viscosity increase in water-based nanofluids not only for the nanofluids presently investigated but also for other results from literature to some extent. As the pH values, particle sizes, and methods of preparation of nanofluids vary in literature and some are not reported precisely, exact predictions are not possible. For example, deviations for the results of Pak and Cho<sup>10</sup> are due to the fact that the particle size used is very small (13 nm) so that the primary viscous coefficient value of  $p$  will be higher. Pak and Cho<sup>10</sup> in their rheological studies, observed a viscosity increase of more than 350 times at 3.5 vol % concentration. Assuming some agglomeration for the above particles, an average value of 60–80 is obtained for the primary viscous coefficient of the present analysis which approximately predicts the above observation. It is seen that a majority of water-based alumina nanofluids results reported in literature exhibit viscosity ratio variation as proposed in Eq. (8). This is mainly due to the fact that majority of nanoparticles used in literature fall under 50–150 nm size range and also due to the fact that most of the commercial alumina nanopowders have an acidic surface and mere mixing of these with water would result in a stable solution electrostatically. Similarly, in the case with ethylene glycol-based nanofluids where the viscosity increase is primarily due to the aggregation of particles, a proper knowledge on the sizes of aggregates present in the solution should be known. It may be noted that in most cases particle aggregation occurs in a suspension; the increase in viscosity may be due the combined effects of electroviscous forces and particle aggregation. Thus from this analysis, it may be emphasized that the understanding of electroviscous effect is equally important as

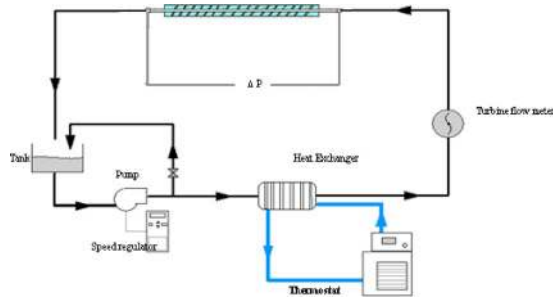


FIG. 10. (Color online) Schematic of setup used for pressure drop measurement studies.

understanding the particle agglomeration effect and it cannot be neglected for suspensions that are electrostatically stabilized.

It is seen from the present study as well as from literature observations that the nanofluids have higher viscosity values when compared to their base fluids. So before putting these fluids for flow applications, evaluation of pressure drops occurring while using them as heat transfer is important. In Sec. III, a flow behavior of nanofluids at room temperature (20 °C) for different volume fractions along is analyzed.

### III. HYDRODYNAMIC EXPERIMENT

The test section used for evaluating pressure drop using hydrodynamic experiments consists of a 1.3 mm inner diameter tube with length of 600 mm through which the nanofluid is circulated. The circulation loop consist of a vane pump (Speck Pump DS-300), followed by a cooling chamber, turbine flow meter (KEM, MH3E/4), and a collecting tank. The schematic of the loop used is shown in Fig. 10. The turbulent flow in the loop is maintained and varied with the help of a pump whose flow rate is precisely controlled by a speed controller (Danfoss VLT 2800) attached to the pump. Pressure drop across the test section tube is measured using a pressure transducer (Contrans ASD800, in three different pressure ranges, viz.,  $\pm 400$ ,  $\pm 2.5$ , and 0–10 bars). A heat exchanger is provided before the test section so as to maintain a constant inlet temperature and to negate any frictional heating occurring at higher flow rates.

Figure 11(a) shows pressure drop values for alumina-water nanofluids which shows that the pressure drop increases with particle loading under the turbulent flow regime (Reynolds number for present flow is in the range of 4500–15 000). Nondimensional form of pressure drop variation with velocity for the above alumina-water nanofluids is shown in Fig. 11(b). Here the friction factor and the Reynolds number are evaluated using the following expressions:

$$f = \frac{2\Delta PD}{\rho LV^2}, \quad (10)$$

$$\text{Re}_D = \frac{\rho VD}{\eta}, \quad (11)$$

where  $\rho$  is density,  $V$  is the velocity,  $D$  is diameter of the tube, and  $L$  is length of the tube.  $\eta$  is the effective viscosity

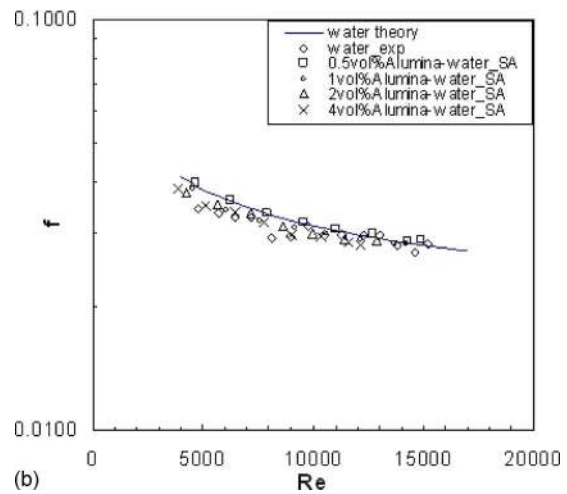
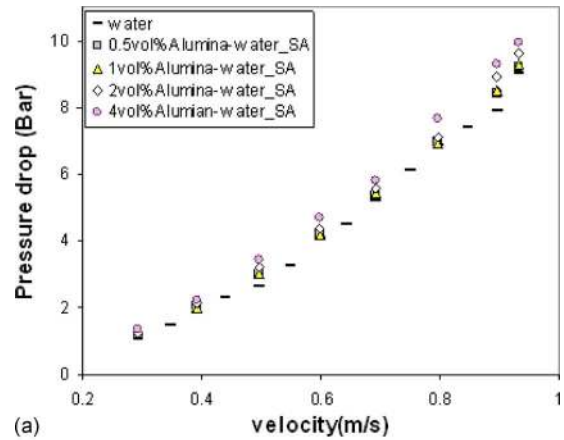


FIG. 11. (Color online) (a) Pressure drop for alumina-water nanofluids with varying velocities. (b) Nondimensional pressure drop and velocity variation for alumina-water nanofluids.

of fluid and measured values from Sec. II C is used for calculation. The density of nanofluids is evaluated using the averaged volume fraction ratio which is generally acceptable, which is given below,

$$\rho_{nf} = (1 - \phi)\rho_{bf} + \phi\rho_p. \quad (12)$$

It may be noted in Fig. 11(b) that the Re value for nanofluid flowing at the same velocity will be lower than that of the base fluid owing to the higher viscosity of the nanofluid. Thus evaluation of flow characteristics at a constant Re value may bring out misleading results as flow properties such as density and viscosity are involved in the evaluation. So care should be taken while interpreting data from nondimensional plots of nanofluids and it would be preferred to have a dimensional plot rather than a nondimensional one as the latter gives more physical insights. The maximum uncertainty in  $f$  and Re were calculated to be 4% and 4.5%, respectively, for the above case.

As physically observed, nanofluids are well dispersed and stable, an approximation of its flow behavior to a homogeneous fluid is well acceptable. Thus efforts are now made to predict the pressure drop based on conventional flow equations. The theoretical evaluation of pressure drop is done using Eq. (10) with friction factors for laminar and turbulent flow regimes as

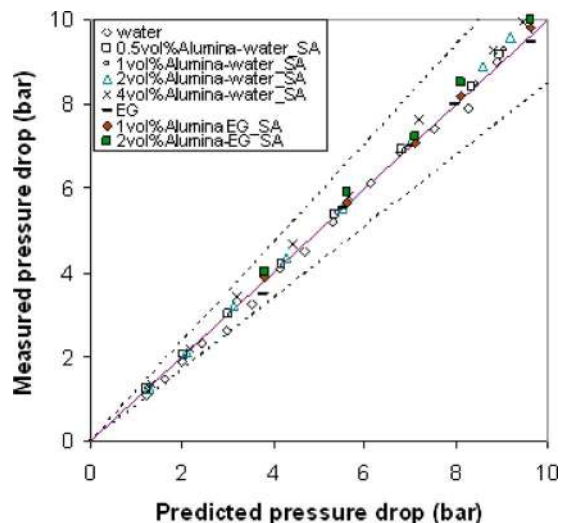


FIG. 12. (Color online) Parity plot between measured and predicted pressure drops.

$$f = \frac{64}{\text{Re}} \quad \text{for } \text{Re} < 2300,$$

$$f = (0.79 \ln \text{Re}_D - 1.64)^{-2} \quad \text{for } \text{Re} > 2300. \quad (13)$$

Figure 12 shows the parity plot between measured and predicted pressure drops. It is seen here that the measured values lie within 15% of the predicted values with all uncertainties included. The above observation also reveals the fact that nanofluids behaves almost like a homogeneous fluids, and by knowing their properties, such as viscosity and density, pressure drop can be predicted accurately.

#### IV. CONCLUSIONS

Thus based on the experiments conducted and data collected from literature, it is observed that the electroviscous effects caused by stabilization procedure are important to be considered and can influence viscosity increase for water-based nanofluids and cannot be neglected at least for suspensions that are electrostatically stabilized. Particle agglomeration is also found to be important and proper particle size distribution curve of the nanofluid should give an estimate of it. Newtonian behavior is exhibited for both water-based and

ethylene glycol-based nanofluids for the particle concentration considered (0.5–6 vol %). Further from pressure drop experiments it is seen that nanofluids behaves like homogeneous fluid and knowing the properties can help in estimating the flow characteristics.

#### ACKNOWLEDGMENTS

The authors would like to thank Deutscher Akademischer Austausch Dienst (DAAD) for providing financial support through the exchange program for K.B.A. We also acknowledge the technical advise given by Professor M. V. Sangaranarayanan, IIT Madras, during the writing of this paper.

- <sup>1</sup>S. K. Das, N. Putra, P. Thiesen, and W. Roetzel, *Int. J. Heat Mass Transfer* **46**, 851 (2003).
- <sup>2</sup>J. Garg, B. Poudel, M. Chiesa, J. B. Gordon, J. J. Ma, J. B. Wang, Z. F. Ren, Y. T. Kang, H. Ohtani, J. Nanda, G. H. McKinley, and G. Chen, *J. Appl. Phys.* **103**, 074301 (2008).
- <sup>3</sup>R. Prasher, D. Song, and J. Wang, *Appl. Phys. Lett.* **89**, 133108 (2006).
- <sup>4</sup>S. M. S. Murshed, K. C. Leong, and C. Yang, *Int. J. Therm. Sci.* **47**, 560 (2008).
- <sup>5</sup>J. Lee, K. S. Hwang, S. P. Jang, B. H. Lee, J. H. Kim, S. U. S. Choi, and C. J. Choi, *Int. J. Heat Mass Transfer* **51**, 2651 (2008).
- <sup>6</sup>H. Chen, Y. Ding, Y. He, and C. Tan, *Chem. Phys. Lett.* **444**, 333 (2007).
- <sup>7</sup>Y. He, Y. J. H. Chen, Y. Ding, D. Cang, and H. Lu, *Int. J. Heat Mass Transfer* **50**, 2272 (2007).
- <sup>8</sup>X. Wang, X. Xu, and S. U. S. Choi, *J. Thermophys. Heat Transfer* **13**, 474 (1999).
- <sup>9</sup>S. E. B. Maïga, C. T. Nguyen, N. Galanis, G. Roy, T. Maré, and M. Coqueux, *Int. J. Numer. Methods Heat Fluid Flow* **16**, 275 (2006).
- <sup>10</sup>P. C. Pak and Y. I. Cho, *Exp. Heat Transfer* **11**, 151 (1998).
- <sup>11</sup>Y. Hwang, Y. Lee, J. Lee, Y. Jeong, S. Cheong, Y. Ahn, and S. H. Kim, *Powder Technol.* **186**, 145 (2008).
- <sup>12</sup>E. Müller and C. Oestereich, *Handling of Highly Dispersed Powders* (Shaker, Aachen, 2004).
- <sup>13</sup>E. Ghzaoui, *J. Appl. Phys.* **86**, 5894 (1999).
- <sup>14</sup>G. K. Batchelor, *J. Fluid Mech.* **83**, 97 (1977).
- <sup>15</sup>A. Einstein, *Ann. Phys.* **34**, 591 (1911).
- <sup>16</sup>Y. Adachi, K. Nakaishi, and M. Tamaki, *J. Colloid Interface Sci.* **198**, 100 (1998).
- <sup>17</sup>V. M. Smoluchowski, *Kolloid-Z.* **18**, 90 (1916).
- <sup>18</sup>J. D. Sherwood, *J. Fluid Mech.* **111**, 347 (1981).
- <sup>19</sup>Y. L. Wang, *J. Colloid Interface Sci.* **32**, 633 (1970).
- <sup>20</sup>F. Booth, *Proc. R. Soc. London, Ser. A* **203**, 533 (1950).
- <sup>21</sup>R. C. D. Cruz, J. Reinshagen, R. Oberacker, A. M. Segadães, and M. J. Hoffmann, *J. Colloid Interface Sci.* **286**, 579 (2005).
- <sup>22</sup>F. J. Rubio-Hernández, M. F. Ayúcar-Rubio, J. F. Velázquez-Navarro, and F. J. Galindo-Rosales, *J. Colloid Interface Sci.* **298**, 967 (2006).